**Atmospheric
Chemistry
and Physics
Discussions**

Classification and investigation of Asian aerosol properties

T. Logan[1], B. Xi[1], X. Dong[1,2], Z. Li[3], and M. Cribb[3]

[1]Department of Atmospheric Science, University of North Dakota, Grand Forks, ND, USA
[2]GCESS, Beijing Normal University, Beijing, China
[3]Department of Atmospheric and Oceanic Science, University of Maryland, College Park, MD, USA

Correspondence to: B. Xi (baike@aero.und.edu)

**Classification and
investigation of Asian
aerosol properties**

T. Logan et al.

Title Page

Abstract	Introduction
Conclusions	References
Tables	Figures

|◀ ▶|
◀ ▶

Back Close

Full Screen / Esc

Printer-friendly Version

Interactive Discussion

Abstract

Ongoing urbanization and industrialization in East Asia have generated a wide variety of aerosols in the atmosphere and have consequently added more uncertainty when evaluating global climate change. To classify different types of aerosols and investigate their physical and chemical properties, four AErosol RObotic NETwork (AERONET) sites have been selected to represent aerosol properties dominated by mixed complex particle types (Xianghe and Taihu), desert-urban (SACOL), and biomass (Mukdahan) over East Asia during the 2001-2010 period. The volume size distribution, aerosol optical depth [$\tau(\lambda)$ and $\tau_{abs}(\lambda)$], Ångström exponent (α and α_{abs}), and the single scattering co-albedo [$\omega_{oabs}(\lambda)$] and $\alpha(\omega_{oabs})$ parameters over the four selected sites have been analyzed. These parameters are used to (a) investigate the aerosol properties and their seasonal variations over the four selected sites, (b) discern the different absorptive characteristics of BC, OC, and mineral dust particles using $\alpha_{abs440-870}$ and $\alpha(\omega_{oabs440-870})$, and (c) develop an aerosol clustering method involving $\alpha_{440-870}$ and $\omega_{oabs440}$. A strong mineral dust influence is seen at the Xianghe, Taihu, and SACOL sites during the spring months (MAM) as given by coarse mode size distribution dominance, declining $\alpha_{440-870}$, and elevated $\alpha_{abs440-870}$ and $\alpha(\omega_{oabs440-870})$ values. A weakly absorbing pollution (OC and biomass) aerosol dominance is seen in the summer (JJA) and autumn (SON) months as given by a strong fine mode influence, increasing $\alpha_{440-870}$, and declining $\alpha_{abs440-870}$ and $\alpha(\omega_{oabs440-870})$ values. A winter season (DJF) shift toward strongly absorbing BC particles is observed at Xianghe and Taihu (elevated $\alpha_{440-870}$, increase in $\alpha_{abs440-870}$ and $\alpha(\omega_{oabs440-870})$). At Mukdahan, a fine mode biomass particle influence is observed year round as given by the volume size distribution, elevated $\alpha_{440-870}$ (higher than the other sites), low $\alpha_{abs440-870}$ and negative $\alpha(\omega_{oabs440-870})$ values indicating weakly absorbing OC particles. The $\alpha(\omega_{oabs})$ parameter is also shown to have less overlap in values than α_{abs} in discerning influences from OC, BC, biomass and mineral dust particles. The clustering method using $\alpha_{440-870}$ and $\omega_{oabs440}$ illustrates four groups of aerosols: Cluster I – fine mode, weakly

Full Screen / Esc

Printer-friendly Version

Interactive Discussion

absorbing pollution particles, Cluster II – fine mode, strongly absorbing pollution particles, Cluster III – coarse mode, strongly absorbing mineral dust particles, and Cluster IV – biomass particles with similar characteristics as Cluster II but less absorbing. This method has shown that aerosol mixtures are both seasonal and regional combinations of particles that were either locally generated or transported from other source regions and should be implemented over other AERONET sites in the future.

1 Introduction

Aerosols originating from the Asian continent have been studied over recent decades and continue to be of great importance due to their varying nature. Ongoing urbanization and industrialization in Asia have generated a wide variety of aerosols in the atmosphere and have consequently added more uncertainty when evaluating global climate change (Hansen and Sato, 2001; Bergstrom et al., 2007; Eck et al., 2010). In addition, mineral dust and biomass burning episodes can also contribute to the total aerosol loading in the atmosphere (Li et al., 2007a, b; Dubovik et al., 2002). Asian dust episodes are more probable and intense during the spring months (Logan et al., 2010; Li et al., 2007b; Huang et al., 2008; Eck et al., 2005) while biomass burning events generally occur as a result of deforestation, agricultural activities, and natural wildfires (Reid et al., 1999; Eck et al., 1999; Boonjawat, 2008; Jeong et al., 2011).

Studies have shown how different aerosol particles can interact during transport (Eck et al., 2005, 2010; Schuster et al., 2005). These particles can combine physically (by impaction or coating) and in some cases chemically (heterogeneous reactions) with one another thus altering their scattering and/or absorptive capabilities (Levin et al., 1996; Schuster et al., 2005; McNaughton et al., 2009; Reid et al., 1999; Streets et al., 2007). Strongly absorptive particles containing black carbon (BC) absorb across much of the solar spectrum (between 0.38 and 1 µm) (Schuster et al., 2005; Lack and Cappa, 2010). Weakly absorptive particles containing organic carbon (OC) absorb across some parts of the UV and visible wavelengths while sulfate particles

predominantly scatter across most wavelengths depending on ambient relative humidity (Eck et al., 2005; Lewis et al., 2008). As a result, the influences of the two different types of aerosols ultimately act as negative radiative forcing agents by reducing the amount of direct downwelling solar radiation to the surface creating a cooling effect

5 (Li et al., 2007a, b; Bergstrom et al., 2007). In addition, aerosols also indirectly affect climate by altering cloud microphysical properties such as cloud albedo, lifetime and precipitation (Li et al., 2007a, b; IPCC, 2007).

The varying composition of the particles within aerosol events is often difficult to measure directly and thus has to be inferred from their physical and chemical proper-

10 ties, in addition to noting their seasonal dependence and variation (Gobbi et al., 2007; Russell et al., 2010; Eck et al., 2005; Li et al., 2007b; Schuster et al., 2005; Dubovik et al., 2002). Recent research has emphasized that quantifying aerosol effects on climate change requires much information on not just the measurements of aerosol loading but also on their physico-chemical properties (i.e., physical properties due to their chemical

15 composition) (Russell et al., 2010; Kaufman et al., 2002; Dubovik et al., 2002; Lewis et al., 2008). Rather than focusing solely on particle size and concentration as a measure for aerosol climactic effects, physico-chemical properties can be derived from their absorptive properties (Russell et al., 2010; Schuster et al., 2005; Dubovik et al., 2002; Bergstrom et al., 2007; Lack and Cappa, 2010).

20 Previous studies have suggested that it is possible to reduce the ambiguities in identifying aerosol composition by using quantities derived from aerosol optical depth ($\tau(\lambda)$), aerosol absorption optical depth ($\tau_{abs}(\lambda)$), Ångström exponent (α), and the single scattering albedo ($\omega_o(\lambda)$) (Russell et al., 2010; Lewis et al., 2008; Bergstrom et al., 2007; Higurashi and Nakajima, 2002). These methods, however, are dependent upon the

25 total volume extinction (β_{ext}) of all particles present in an aerosol mixture. This can introduce some uncertainties in identifying the predominant aerosol composition in a mixture because pollution particles (sulfates, OC, and BC) can have similar size distributions and $\tau(\lambda)$ values but not necessarily the same internal properties (Schuster et al., 2005; Higurashi and Nakajima, 2002).

Four Asian AERONET sites (Xianghe, Taihu, SACOL, and Mukdahan) have been selected for this study because they are periodically affected by a combination of pollution, biomass burning and mineral dust particles (Boonjawat, 2008; Eck et al., 2003; Eck et al., 2005; Xin et al., 2007; Bi et al., 2010). For example, Eck et al. (2005) found good agreement between the Beijing and Xianghe AERONET data sets in the 2001 spring season and suggested that Xianghe can be influenced by mineral dust and locally generated pollution as well as biomass particles from Russia. Xin et al. (2007) used $\tau_{500\,nm}$ and $\alpha_{440-650}$ to discern different aerosol types in several Chinese cities including Xianghe, Taihu (Lake Tai), and Lanzhou while Bi et al. (2010) used $\tau_{500\,nm}$, $\alpha_{440-870}$, ω_o, and refractive index to show how the SACOL site was seasonally influenced by contributions from both dust and anthropogenic aerosols. Mukdahan is a poorly characterized region with few studies, however, the Eck et al. (2003) and Boonjawat (2008) studies did show biomass and anthropogenic aerosol influences using AERONET observations.

This study reports the relative influence and seasonal aerosol dependence at four Asian AERONET sites and focuses primarily on the absorptive properties of aerosols to further examine and classify particle types in an aerosol mixture. We employ the use of the volume size distribution as well as the $\tau_{440\,nm}$, $\tau_{abs440\,nm}$, α, and α_{abs} parameters, as well as two quantities derived from the single scattering albedo [($\omega_o(\lambda)$]: the single scattering co-albedo (1-$\omega_o(\lambda)$ or $\omega_{oabs}(\lambda)$) and the $\alpha(\omega_{oabs})$. This is different than the other studies in that the latter two parameters will be used to investigate how the absorptive nature of the aerosols varies as a function of season, physical and chemical processes (e.g., internal/external mixing, secondary reactions and combustion phase), and source region. A discussion of the methodology used in the retrieval and usage of AERONET observations as well as calculating the $\alpha(\omega_{oabs})$ parameter is outlined in Sect. 2. The seasonal variations of aerosol size and absorptive properties are presented and discussed in Sect. 3. The feasibility of using the $\omega_{oabs}(\lambda)$ and α parameters in a cluster analysis is also discussed in Sect. 3. The final section includes a brief summary and conclusion of our results.

2 Data and methodology

2.1 AERONET

The AErosol RObotic NETwork (AERONET) consists of CIMEL sun/sky radiometers placed in a world-wide framework of observation stations (Holben et al., 1998). The instruments are capable of retrieving aerosol optical property products at discrete wavelengths ranging from 340 to 1020 nm (Schuster et al., 2006; Eck et al., 2004). This study uses Level 2.0 (cloud screened, quality assured) products to ensure data quality and accuracy (Holben et al., 2006). The aerosol products were generated using the inversion techniques developed by Dubovik and King (2000) and Dubovik et al. (2000), and quality assurance using Holben et al. (2006). Daily averaged data collected from the four AERONET sites span the following years: 2001–2010 (Xianghe), 2005–2010 (Taihu), 2006–2011 (SACOL), and 2003–2009 (Mukdahan).

The AERONET products analyzed in this study include: single scattering albedo ($\omega_o(\lambda)$, λ between 440 nm and 870 nm), aerosol optical depth, ($\tau(\lambda)$, λ between 440 nm and 870 nm), particle effective radius (r_{eff}), and the volume particle size distribution. We use $\tau(\lambda)$ and $\omega_o(\lambda)$ to calculate the τ_{abs440}, $\alpha_{440-870}$, $\alpha_{abs440-870}$, and $\omega_{oabs440}$ parameters, and ω_{oabs} (440–870 nm) to calculate the $\alpha(\omega_{oabs440-870})$ parameter. The uncertainties of $\tau(\lambda)$ and ω_o are approximately ±0.01 and ±0.03, respectively, for $\tau_{440} > 0.4$ (Holben et al., 1998; Eck et al., 1999; Dubovik et al., 2002). Though this threshold may bias our results, our conclusions are not greatly affected using $\tau_{440} > 0.4$. It should be noted that the AERONET observations are usually discontinuous and may only contain one almucantar in a day, thus a summary of number of samples over the four selected sites is listed in Table 1.

AERONET sites

The locations of the four selected AERONET sites: Xianghe (39.75° N, 116.96° E), Taihu (31.4° N, 120.21° E), and SACOL (35.95° N, 104.14° E) in China, and Mukdahan,

Thailand (16.61° N, 104.68° E), are shown in Fig. 1. Xianghe is located in a mixture region and influenced by pollution, biomass burning and mineral dust particles (Eck et al., 2005, 2010; Logan et al., 2010). The other three sites represent an urban region (Taihu), a desert-urban region (SACOL) and a biomass dominant region (Mukdahan).

Taihu is located in a region heavily influenced by airflow from large urban centers (e.g., Shanghai and Hangzhou) and industry in each cardinal direction and to a lesser extent, the influences of the Gobi and Taklimakan Deserts (Xin et al., 2007). SACOL, the Semi-Arid Climate and Environment Observatory of Lanzhou University, is situated in central China (Gansu province) within the reaches of the Loess Plateau (downwind of Gobi

and Taklimakan Deserts) (Huang et al., 2008). The site is just southeast of Lanzhou City, a large metropolitan and industrial center ($\sim$ 3.5 million inhabitants). Mukdahan is located in extreme eastern Thailand near the Laotian border where crop and vegetation burning is prominent during the dry season (Boonjawat, 2008).

2.2 Aerosol classification methodology

2.2.1 Aerosol optical depth, Ångström exponent, and spectral variation

Aerosol optical depth ($\tau(\lambda)$) is the integral quantity of the optical path (or extinction, β_{ext}) of a solar photon passing through a layer medium (i.e., aerosol layer) and is the sum of the scattering and absorption optical depths of the medium (Eck et al., 1999). $\tau(\lambda)$ can be measured from many observational platforms (e.g., ground based, sub-orbital in situ, and space based) and is used as a primary parameter in quantifying the magnitude of aerosol loading in an atmospheric column (Holben et al., 1998; Eck et al., 1999; Li et al., 2007a, b). The Angström exponent, α, is a good indicator of the size of particles and is given by the following equation,

$$\alpha = -\frac{\ln\left[\frac{\tau(\lambda_1)}{\tau(\lambda_2)}\right]}{\ln\left[\frac{(\lambda_1)}{(\lambda_2)}\right]}, \tag{1}$$

where the log-slope relationship between τ and λ is synonymous with wavelength dependence due to particle size (Eck et al., 1999; Schuster et al., 2006). The wavelength range used in this study is 440 nm to 870 nm. Similar to the Higurashi and Naka-jima (2002) study, we adopt $\alpha_{440-870} < 0.8$ to denote coarse mode particles (weak wavelength dependence) and $\alpha_{440-870} > 0.8$ to denote fine mode particles (strong wavelength dependence). $\alpha_{440-870}$ can be negative (strong mineral dust influence) or surpass values greater than 2 (OC, BC, and biomass particles) (Higurashi and Naka-jima, 2002; Gobbi et al., 2007; Eck et al., 1999). The spectral variation of Angström exponent ($\delta\alpha$) or slope of α is given by the expression,

$$\delta\alpha = \alpha_{440,675\,nm} - \alpha_{675,870\,nm}. \tag{2}$$

Studies including our previous study (Logan et al., 2010) reported the usefulness of this parameter in discerning the relative influences of both fine ($\delta\alpha < 0$) and coarse ($\delta\alpha \sim 0$) mode particles in an aerosol mixture (Eck et al., 1999; Gobbi et al., 2007; Basart et al., 2009; Schuster et al., 2006).

In the Logan et al. (2010) study, we tracked the physical and optical properties of aerosol events originating from various source regions in Asia, and discussed their transpacific transport to the sink region in North America. We used $\delta\alpha$ to illustrate the dominant particle mode of aerosol events and found three types: (a) dust dominant (from arid/desert areas), (b) pollution dominant (from large urban centers in central and eastern Asia), and (c) mixture of dust and pollution. We used back trajectory analysis to confirm the origins of the events since little was known about their composition before they exited the Asian mainland. Additionally, we found an overlap among the pollution type particles (e.g., biomass burning, OC and BC aerosols) which had similar values for both α and $\delta\alpha$. This study plans to build upon the conclusions of our previous study by investigating the different particle influences from the source region.

2.2.2 Volume size distribution, ω_o, τ_{abs}, ω_{oabs}, α_{abs}, and $\alpha(\omega_{oabs})$

We use the volume particle size distribution as a general fingerprint for each particle generation region (Dubovik et al., 2002; Eck et al., 2005). Bimodal distributions tend to suggest more than one type of aerosol and the total volume of either the coarse or fine modes will indicate the dominance of a particular type in that region (Dubovik et al., 2002). However, this does not give information on particle composition since pollution and biomass particles can yield similar distributions.

The single scattering albedo (ω_o) (ratio of scattering to extinction aerosol optical depths) can infer particle composition (pollution, mineral dust, and biomass) by exploiting the spectral dependence of particle absorption with wavelength (Eck et al., 1999; Corrigan et al., 2006). The single scattering co-albedo (1-ω_o or ω_{oabs}) (ratio of absorption to extinction aerosol optical depths) explains the loss of photons to absorption which is also useful in identifying particle composition (Corrigan et al., 2006). Many studies have employed the use of the α_{abs} parameter to (a) reduce ambiguities in aerosol composition and (b) reveal a correlation between α_{abs} and aerosol composition (e.g., Russell et al., 2010; Bergstrom et al., 2002, 2007; Eck et al., 2010; Giles et al., 2011). They calculated α_{abs} starting with the absorption aerosol optical depth, $\tau_{abs}(\lambda)$, given by

$$\tau_{abs}(\lambda) = (1 - \omega_o(\lambda)) * \tau(\lambda), \tag{3}$$

where we use λ at 440 and 870 nm. They then used the same equation for α (Eq. 1 and same λ range) to calculate α_{abs}

$$\alpha_{abs} = -\frac{\ln\left[\frac{\tau_{abs}(\lambda_1)}{\tau_{abs}(\lambda_2)}\right]}{\ln\left[\frac{(\lambda_1)}{(\lambda_2)}\right]}. \tag{4}$$

A range of $\alpha_{abs440-870}$ values has been previously determined which corresponds to various aerosol types. For weakly absorbing particles (e.g., non-refractory OC particles), the $\alpha_{abs440-870}$ values are near or below one (Russell et al., 2010), while for

strongly absorbing particles, the values vary significantly. For example, urban pollution particles (e.g., BC, OC, and sulfates) typically have $\alpha_{abs440-870}$ from ~ 1 (BC dominant) to 2 or greater (OC dominant), while mineral dust particles can be 1.5 or higher depending on composition (Giles et al., 2011; Lack and Cappa, 2010; Russell et al.,

5   2010; Xin et al., 2007; Schuster et al., 2005). Although $\alpha_{abs440-870}$ can be used to discern various aerosol types, it has a limitation, in particular when different aerosols having similar wavelength dependence are mixed with one another (Lack and Cappa, 2010; Higurashi and Nakajima, 2002).

We explore the feasibility of the single scattering co-albedo [$\omega_{oabs}(\lambda)$] parameter in

10   place of $\tau_{abs}(\lambda)$ in Eq. (4) to calculate the $\alpha(\omega_{oabs})$ parameter given by

$$\alpha(\omega_{oabs}) = -\frac{\ln\left[\frac{\omega_{oabs}(\lambda_1)}{\omega_{oabs}(\lambda_2)}\right]}{\ln\left[\frac{(\lambda_1)}{(\lambda_2)}\right]}, \tag{5}$$

where the 440 nm and 870 nm wavelengths are used. We use this parameter to explain aerosol absorptive behavior in low mean $\tau_{440\,nm}$ conditions (e.g., mineral dust regions). Though this parameter does not directly depend on $\tau(\lambda)$ and hence particle size infor-

15   mation (Eq. 3), it is still derived from $\tau(\lambda)$ and sky radiance retrievals and has the same limitations and uncertainties, therefore we limit data to retrievals involving $\tau_{440\,nm} > 0.4$ (Dubovik and King, 2000; Dubovik et al., 2002; Eck et al., 2005).

3   Modeled vs. observed wavelength dependence of τ and τ_{abs}

Since aerosols exist as complex mixtures, especially in Asia, theoretical models can

20   aid in understanding observed aerosol behavior. If aerosol properties for pure aerosols are known, they can then serve as a baseline or ground truth to analyze the observed aerosol properties, particularly for a mixture of aerosols. The model outputs from the Yoon et al. (2011) study illustrated the theoretical wavelength dependence of $\tau(\lambda)$ and

$\tau_{abs}(\lambda)$ (440 nm $< \lambda <$ 1020 nm) for pollution, mineral dust and biomass type particles. Mineral dust particles are shown to have a weak wavelength dependence on $\tau(\lambda)$ yet strong wavelength dependence in the visible for $\tau_{abs}(\lambda)$. Biomass particles have a strong wavelength dependence in $\tau(\lambda)$ but intermediate dependence on $\tau_{abs}(\lambda)$ with
5   some overlap with pollution. Pollution type particles have an intermediate $\tau(\lambda)$ dependence but strong $\tau_{abs}(\lambda)$ dependence at all wavelengths.

Figure 2 shows the statistical results of normalized aerosol extinction and absorption optical depths retrieved from the four selected sites. The $\tau(\lambda)$ wavelength dependences at the four selected sites are in good agreement with the model outputs indicating
10   the dominant aerosol type at each site. SACOL has the weakest wavelength dependence of all four sites due to coarse mode particle dominance, while Mukdahan has the strongest wavelength dependence due to fine mode particles. Xianghe and Taihu have an intermediate dependence due influences from both coarse and fine mode particles.

For $\tau_{abs}(\lambda)$, the results from the four selected sites are slightly different than the model
15   outputs. Over the wavelengths from 440 to 1020 nm, Mukdahan has the weakest $\tau_{abs}(\lambda)$ wavelength dependence due to weakly absorbing OC particles generated as a result of combustion phase and moisture content (Reid et al., 1999; Andreae and Gelencsér, 2006). Xianghe and Taihu have the strongest (absorption) wavelength dependence while SACOL has an intermediate (absorption) wavelength dependence. The charac-
20   teristics of $\tau_{abs}(\lambda)$ wavelength dependence are changed slightly when the wavelength is broken into two parts: visible (440–675 nm) and longer one (675–1020 nm). In the visible band, the absorption at SACOL is nearly the same as those at both Xianghe and Taihu, but much stronger than the absorption at Mukdahan. In the longer band, however, the absorption at SACOL is much weaker than those at other three sites.

25   The discrepancies between modeled and observed $\tau_{abs}(\lambda)$ can be attributed to the complex aerosol mixtures over four selected sites, while model calculations only account for pure aerosols. For example, Xianghe and Taihu have the strongest wavelength dependence attributed to influences from a variety of strongly absorbing aerosol types (BC and mineral dust) (Zheng et al., 2005; Xin et al., 2007). At SACOL, mineral

dust can have varying amounts of iron (e.g., hematite) as well as anthropogenic influences (OC and BC) (Koven and Fung, 2006; Xin et al., 2007). It appears the extinctive properties of aerosol mixtures can be well modeled because they are dominated by the aerosol scattering properties, however, the absorptive properties are difficult to model and we therefore use volume size distribution and parameters based upon a combination of $\tau(\lambda)$, $\tau_{abs}(\lambda)$, $\omega_o(\lambda)$, and $\omega_{oabs}(\lambda)$ to further discern the various particle influences in Asian aerosol mixtures.

4 Results and discussions

We employ five aerosol parameters: τ_{440}, τ_{abs440}, $\alpha_{440-870}$, $\alpha_{abs440-870}$, and $\alpha(\omega_{oabs440-870})$ along with the volume size distribution in order to describe the physicochemical properties of aerosol events over the four selected AERONET sites. We analyze and discuss the annual and seasonal volume size distributions in Sect. 4.1 and monthly means of τ_{440}, τ_{abs440}, $\alpha_{440-870}$, $\alpha_{abs440-870}$, and $\alpha(\omega_{oabs440-870})$ in Sect. 4.2. These two sections lay a foundation for the discussion of our classification method involving the use of $\alpha_{440-870}$ and $\omega_{oabs440}$ in Sect. 4.3. The annual and seasonal means, as well as other statistical results, are listed and summarized in Table 1.

4.1 Annual and seasonal aerosol size distributions

Figure 3 shows the annual and seasonal averaged volume aerosol size distributions from the four selected AERONET sites. As illustrated in Fig. 3a both the Xianghe and Taihu sites show a bimodal distribution with a fine mode peak of 0.16 µm and coarse mode peak near 3 µm. The Xianghe site shows an overall larger coarse than fine mode influence due to the close proximity to the Gobi desert mineral dust source regions, aggregates of pollution type aerosols (e.g., BC, soot, aged biomass aerosols), and other coarse mode particles advected in from surrounding areas (Zheng et al., 2005; Streets et al., 2007). Taihu has equal contributions of fine and coarse mode aerosols

due to numerous nearby industrial and urban pollution sources as well as hygroscopic growth of aerosols (Yao et al., 2002; Pathak et al., 2009; Jin et al., 2011; Li et al., 2007a; Eck et al., 2005). The SACOL site is generally unimodal with a coarse mode peak of 2.1 µm indicative of mineral dust influences, however, not always of the same origins as Xianghe (Huang et al., 2008). Mukdahan is a near mirror image of SACOL with a largely unimodal fine mode peak at 0.2 µm (strong biomass influence). Though Fig. 3a shows the annual mean variations of aerosol size distribution, the seasonal variations are needed in order to investigate any possible periodic dependence of aerosol generation.

Figure 3b–e suggest that three of the four sites had coarse mode dominance during the spring season due to aerosol influences from the Gobi (Xianghe and Taihu) and Taklimakan (SACOL) Deserts (Huang et al., 2008). The summer season shows a change in aerosol size dominance from coarse to fine mode. The wet monsoon also begins during this time period which in turn enables southerly winds to transport pollution (BC, OC, and biomass) and moisture from the lower latitudes of southern and eastern Asia northward (Fig. 1). The increased humidity creates an abundance of suspended water vapor molecules to absorb and adsorb on the polluted aerosols. SACOL also has a slightly larger fine mode during summer season than during spring season, which suggests a pollution influence in this region (Huang et al., 2008). Mukdahan appears to be influenced by biomass burning activity throughout the dry season from numerous wildfires and ongoing agricultural activities (Boonjawat, 2008). It should be noted that due to wet monsoon activity the Taihu and Mukdahan sites have only limited observations of aerosols, especially during the summer months (Eck et al., 2005; Boonjawat, 2008).

The autumn months (SON) show a decrease in the magnitudes of both fine and coarse mode particles across all sites due to shifts in both type and size except in Mukdahan where the r_{eff} increases from 0.16 µm to 0.25 µm possibly due to hygroscopic growth during this period. At both the Taihu and Xianghe sites, aerosols that either formed from local biomass burning or advected in from neighboring regions may have been responsible for the increase in the volume coarse mode (Eck et al., 2010;

Kondo et al., 2011; Xin et al., 2007). At the SACOL site, the volume contributions from fine mode aerosols are comparable to the coarse mode aerosols though the number concentration is dominated by fine mode aerosols (Huang et al., 2008).

The winter months (DJF) show equal coarse and fine mode aerosol contributions at Taihu while at the Xianghe site, the coarse and fine modes are similar in magnitude as in the autumn months. Aerosol generation from industrial sources is still ongoing in Taihu while aerosols derived from charcoal (e.g., winter residential heating) in Xianghe may explain the coarse mode peak (Xin et al., 2007). Late winter dust activity (Gobi Desert) may have been responsible for the increasing coarse mode influence at SACOL (Huang et al., 2008). In Mukdahan, the fine mode peak shifts towards a smaller r_{eff} (0.17 µm) due to a lack of moisture (no hygroscopic growth) during this period. To further investigate the aerosol properties over the four selected sites, we plot Fig. 4 to illustrate the seasonal variations of five interested aerosol parameters in the following section.

4.2 Seasonal variations of aerosol properties

Figure 4a shows the monthly means of $\tau_{440\,nm}$ at the four selected AERONET sites. Xianghe and Taihu both have summer maxima and late autumn/winter minima in $\tau_{440\,nm}$ which suggest a dependence on factors such as urban/industrial activity, weather patterns, and available moisture (Pan et al., 2010). Taihu has a moderate level of variation in $\tau_{440\,nm}$ due to its proximity to a multitude of industrial aerosol sources that not only emit pollution particles year round but periodically switch fuel type (Xin et al., 2007; Wang et al., 2008). SACOL has maxima in April and June where the spring maximum can be attributed to strong dust activity beginning in early spring lasting to May, while the summer maximum corresponds to industrial influences from Lanzhou that become dominant for the remainder of the year (Huang et al., 2008). In Mukdahan, biomass activity is at a maximum during March with a second maximum in the autumn after the rainy season (Boonjawat, 2008).

The $\tau_{abs440\,nm}$ parameter in Fig. 4b represents particle absorption strength and variability. Xianghe had both the largest $\tau_{abs440\,nm}$ variability (0.045–0.14) and maximum $\tau_{abs440\,nm}$ value (0.14). The summer minima and winter maxima at Xianghe and Taihu indicate that the different pollution particles over these two sites were weakly absorbing during the summer months and strongly absorbing during the winter months. SACOL had near constant $\tau_{abs440\,nm}$ values with mineral dust and pollution particles present through the year except in April when mineral dust particles were a major contributor to $\tau_{440\,nm}$. Mukdahan had low, nearly constant $\tau_{abs440\,nm}$ values, indicating that an abundance of weakly absorbing particles contributed to $\tau_{440\,nm}$. The $\tau_{abs440\,nm}$ values during the period February–March were more than double the other months, suggesting the presence of additional particle types. This may be the result of combustion phase, type of vegetation burned, or aged biomass particles (Dubovik et al., 2002; Kondo et al., 2011).

Figure 4c illustrates the seasonal variation in extinction wavelength dependence $\alpha_{440-870}$ where Xianghe, Taihu, and SACOL had spring minima due to mineral dust particle influence with a more prolonged dust influence period at SACOL. The increase in $\alpha_{440-870}$ during the summer months is due to hygroscopic fine mode sulfate and OC particle influences at Xianghe and Taihu while at SACOL ambient mineral dust mixes with pollution (Lanzhou) thereby keeping the mean $\alpha_{440-870}$ lower than the other sites (Zheng et al., 2005; Xin et al., 2007). The monthly mean $\alpha_{440-870}$ values at Mukdahan are higher than those at the other three sites, especially during the spring months due to biomass particles being the dominant aerosol type (Boonjawat, 2008).

Figure 4d shows the seasonal variation in absorptive wavelength dependence $\alpha_{abs440-870}$ where both Xianghe and Taihu had very similar $\alpha_{abs440-870}$ trends throughout the year except for late spring when the influence of strongly absorbing mineral dust particles lingered longer at Xianghe than Taihu (Gobi Desert influence). Particles at both sites showed a weak wavelength dependence in the summer due to influences from sulfate, OC, biomass aerosols as well as linear combinations of their mixtures. At SACOL, the monthly mean $\alpha_{abs440-870}$ values increase significantly from the winter

to the spring, and reach a maximum in April-May due to the prevalence of mineral dust (Loess Plateau/Taklimakan Desert) at this site. At Mukdahan, the monthly mean $\alpha_{abs440-870}$ values are lower than those from other three sites, indicating that the particles generated from biomass burning activity tend to be weakly absorbing.

It is interesting that $\alpha_{abs440-870}$ values at the SACOL site are lower than at Xianghe and Taihu sites. Though it can be misleading since $\alpha_{abs440-870}$ for dust is typically higher than for pollution, by exploiting the relationship between $\tau_{440\,nm}$ and $\alpha_{abs440-870}$ it can be shown that the low values are attributed to fewer occurrences of cases with high $\tau_{440\,nm}$ in this region (Fig. 4a). Therefore, we investigate the feasibility of using $\alpha(\omega_{oabs440-870})$ in order to aid in resolving this issue.

As indicated in Fig. 4e, the monthly mean $\alpha(\omega_{oabs440-870})$ values at the Xianghe and Taihu sites range between −0.2 (summer/early autumn months) and 0.5 (late autumn/winter). In the spring months, the maximum $\alpha(\omega_{oabs440-870})$ values are well correlated with minimum values of $\alpha_{440-870}$ (Fig. 4c). Though Xianghe and Taihu have similar variability in $\alpha(\omega_{oabs440-870})$, there is more of a separation in mean $\alpha(\omega_{oabs440-870})$ between these two sites (i.e., less overlap). Both sites have a spring maximum (dust activity) and summer minimum (weakly absorbing OC, biomass, and sulfate particles). In fact, the late summer months (August and September) have the lowest $\alpha(\omega_{oabs440-870})$ values which correspond with widespread biomass burning activity advected from nearby farmlands as well as southeast Asia (Eck et al., 2005). The monthly mean $\alpha(\omega_{oabs440-870})$ values during the winter months are slightly higher than those from the summer months because BC emissions from residential heating and industry, in particular at Xianghe, are prevalent during this season (Zheng et al., 2005).

SACOL has a similar spring maximum due to dust activity but the maximum occurs one month after the maximum $\alpha_{abs440-870}$. This may be attributed to the presence of a large amount of floating and blowing dust still present in the region during May (one month after peak dust activity) (Huang et al., 2008; Bi et al., 2010). There are two $\alpha(\omega_{oabs440-870})$ minima in July and November due to possible biomass activity and local pollution, respectively while winter dust activity and BC emissions are responsible

for the increase in $\alpha(\omega_{\text{oabs}440-870})$ (Huang et al., 2008; Xin et al., 2007). In essence, once the dust season abates, pollution from Lanzhou City reasserts itself as the dominant absorbing particle mode. Mukdahan has slightly higher $\alpha(\omega_{\text{oabs}440-870})$ values in the spring than the autumn/winter months due to changes in combustion phase of veg-
5   etation (wildfire vs. controlled burn) and burned vegetation type (Dubovik et al., 2002).

The volume size distribution as well as the $\alpha_{\text{abs}440-870}$ and $\alpha(\omega_{\text{oabs}440-870})$ parameters are useful in identifying regional aerosol characteristics. We find the $\alpha(\omega_{\text{oabs}440-870})$ parameter to be more correlated with particle volume distribution as it more clearly indicates the absorptive properties of mineral dust during the spring
10 (coarse mode dominance) and biomass activity in the summer (fine mode dominance) at the SACOL, Xianghe and Taihu sites. Though the $\alpha(\omega_{\text{oabs}440-870})$ parameter shows a better separation between BC/OC and biomass influences, it still needs more study to better discern between BC and OC particles. However, due to the wide variety of organics produced by combustion as well as secondary particles generated during transport,
15 this will be difficult (Lack and Cappa, 2010). We explore the $\alpha_{440-870}$ and $\omega_{\text{oabs}440-870}$ parameters as a means of further supporting our results by using aerosol cases from regions dominated by pollution, mineral dust, and biomass particles. We then show how the four Asian sites are approximate combinations of the selected regions.

4.3   A cluster method involving $\alpha_{440-870}$ and $\omega_{\text{oabs}440}$

20 Since the four selected sites are dominated by the nature of aerosol mixtures, we have analyzed four additional AERONET sites where each site is primarily composed of a single aerosol type. The purpose of selecting four additional sites is to demonstrate how the cluster method can classify a single type aerosol using $\alpha_{440-870}$ and $\omega_{\text{oabs}440,}$ which will serve as baseline for analyzing the aerosol properties over the four selected
25 sites. In Fig. 5 we present the results of four additional AERONET sites that reflect source regions dominated by pollution [Mexico City (19.34° N, 99.18° W) and NASA Goddard (38.99° N, 76.84° W)], mineral dust [Solar Village (24.91° N, 46.40° E)], and biomass particles [Alta Floresta (9.87° S, 56.10° W)]. In this study, we define Cluster

I as fine mode, weakly absorbing particle dominance while Cluster II as fine mode, strongly absorbing particle dominance. Cluster III represents coarse mode mineral dust aerosol cases and Cluster IV denotes fine mode biomass particles. It should be noted that winter, spring, and summer cases are presented at the Alta Floresta site (Southern
5   Hemisphere).

Figure 6a and b detail three groups of aerosols (i.e., Clusters I, II, and III) at Xianghe and Taihu with Xianghe having more aerosol cases than Taihu. There is a noticeable seasonal dependence in $\alpha_{440-870}$ and $\omega_{oabs440}$ as strongly absorbing aerosol cases ($\omega_{oabs440} > 0.07$) occur primarily during the spring, autumn and winter months
10 while weakly absorbing aerosol cases ($\omega_{oabs440} < 0.07$) occur during the summer with a moderate degree of seasonal overlap. This conclusion is consistent with the results from the previous sections that indicated summer/autumn sulfate, biomass, and OC dominant particles (Cluster I), winter BC and OC aerosols from residential heating and factory emissions (Cluster II), and spring dust activity (Cluster III). The aerosol proper-
15 ties in Clusters I and II at Xianghe are comparable to those at Taihu while the aerosols in Cluster III at Xianghe are slightly more coarse mode (more samples with $\alpha_{440-870}$ ~ 0) and stronger absorbing (more samples with $\omega_{oabs440} > 0.5$) than those at Taihu due to its closer proximity to the Gobi Desert and greater number of dust cases.

There are two distinct aerosol clusters at SACOL (Fig. 6c). Compared to those at Xi-
20 anghe and Taihu, the $\alpha_{440-870}$ and $\omega_{oabs440}$ values in Cluster II at SACOL are smaller, indicating less fine mode and weakly absorbing aerosols over SACOL. Though the aerosol properties in Cluster III are comparable to those at Xianghe, there is an apparent shift towards a lower range of $\omega_{oabs440}$ values (less absorbing) and more samples with $\alpha_{440-870} \sim 0$ (more coarse mode). This is due to the differing regional aerosol in-
25 fluences at both sites since SACOL is located within a dust region with few cities, while Xianghe is in a sub-urban setting surrounded by many large cities and industry as well as being downwind from a desert region (Xin et al., 2007).

Comparing the Cluster IV results at Mukdahan with the Clusters I and II results at Xianghe and Taihu, we conclude that biomass particles represent the mixture of Clusters

Full Screen / Esc

Printer-friendly Version

Interactive Discussion

I and II with larger $\alpha_{440-870}$ and smaller $\omega_{oabs440}$ values (but similar variability) on average (Fig. 6d). The variability here is likely due to a wide variety of OC and BC particles generated by combustion conditions and moisture (Dubovik et al., 2002; Zheng et al., 2005; Reid et al., 1999). There is a seasonal dependence with the winter months having a higher mean $\omega_{oabs440}$ than the spring while the autumn months have more weakly absorptive cases.

The large variability in $\alpha_{440-870}$ and $\omega_{oabs440}$ seen in this clustering method can be problematic due to the overlap of aerosol clusters. However, since similar variabilities were shown at the NASA Goddard, Mexico City, Solar Village and Alta Floresta sites, it is possible that the distribution of aerosol cases seen in this study is not unique to any one region, but is indicative of regions dominated by various aerosol types. In general, the $\alpha_{440-870}$ and $\omega_{oabs440}$ method supports the results discussed in the above sections. Thus a future study is warranted in order to implement this cluster method to other AERONET sites dominated by one or more aerosol types. In time, we can draw a firm conclusion for the versatility of this cluster method.

5 Summary and conclusions

In this study, four AERONET sites have been selected to represent aerosol properties reflecting biomass (Mukdahan), desert-urban (SACOL), and complex mixed particle type (Xianghe and Taihu) influences. The volume particle size distribution and five robust parameters (τ_{440}, τ_{abs440}, $\alpha_{440-870}$, $\alpha_{abs440-870}$, $\alpha(\omega_{oabs440-870})$) have been investigated to show a seasonal dependence on aerosol type and composition at these sites.

Mineral dust influences are clearly seen at Xianghe, Taihu, and SACOL primarily during the spring months (MAM) as illustrated by the large coarse mode volume distribution area, low $\alpha_{440-870}$, and elevated $\alpha_{abs440-870}$ and $\alpha(\omega_{oabs440-870})$. During the summer months (JJA) there is a shift towards more fine mode aerosols derived primarily from anthropogenic sources as given by fine mode dominance, high $\alpha_{440-870}$,

and low $\alpha_{abs440-870}$ and $\alpha(\omega_{oabs440-870})$ values at Xianghe, Taihu, and SACOL. The autumn months (SON) show influences from biomass burning then a shift towards more absorbing aerosols (BC particle influence) at Xianghe and Taihu. During the winter (DJF), BC particles are dominant at Xianghe, Taihu and SACOL as given by high

5   $\alpha_{440-870}$ and elevated $\alpha_{abs440-870}$ and $\alpha(\omega_{oabs440-870})$. Mukdahan has the highest overall $\alpha_{440-870}$, lowest $\alpha_{abs440-870}$ and negative $\alpha(\omega_{oabs440-870})$ values indicating weakly absorbing biomass particles. There is a seasonal dependence in $\alpha_{440-870}$ suggesting varying vegetation types, burning conditions and available moisture.

  We use $\alpha_{440-870}$ and $\omega_{oabs440}$ to show distinct groups of aerosol cases comprised

10   of pollution (weakly and strongly absorbing), mineral dust, and biomass particles. We first apply this method to four additional AERONET sites (NASA Goddard, Mexico City, Solar Village, and Alta Floresta) in order to illustrate the relative contributions and seasonal dependence of aerosol types at the four selected sites used in this study. Both Xianghe and Taihu have three identifiable clusters of aerosol types reflecting the influ-

15   ences of local emissions (Clusters I and II) as well as aerosols advected from outside sources (Cluster III). SACOL also has pollution and mineral dust influences (Clusters II and III) but the aerosol cases are found to be more coarse mode (lower $\alpha_{440-870}$) and less absorptive (lower $\omega_{oabs440}$). Mukdahan has a single cluster (Cluster IV) of aerosols owing to biomass particle influences that were shown to have a seasonal dependence.

20   The results of this study will provide a ground truth to validate satellite retrieved and model simulated aerosol properties. The clustering method using $\alpha_{440-870}$ and $\omega_{oabs440}$ can especially illustrate a broad fingerprint of a region dominated by several different types of aerosol influences and will be used over other AERONET sites in the future.

Classification and investigation of Asian aerosol properties

T. Logan et al.

References

Andreae, M. O. and Gelencsér, A.: Black carbon or brown carbon? The nature of light-absorbing
5   carbonaceous aerosols, Atmos. Chem. Phys., 6, 3131–3148, doi:10.5194/acp-6-3131-2006,
2006.

Bergstrom, R. W., Russell, P. B., and Hingett, P.: Wavelength Dependence of the Absorption of
Black Carbon Particles: Predictions and Results from the TARFOX Experiment and Implica-
tions for the Aerosol Single Scattering Albedo, J. Atmos. Sci., 59, 567–577, 2002.

10   Bergstrom, R. W., Pilewskie, P., Russell, P. B., Redemann, J., Bond, T. C., Quinn, P. K., and
Sierau, B.: Spectral absorption properties of atmospheric aerosols, Atmos. Chem. Phys., 7,
5937–5943, doi:10.5194/acp-7-5937-2007, 2007.

Boonjawat, J.: Impact Assessment of Biomass-burning Aerosols in Southeast Asia, Greater
Mekong Subregion – Core Environmental Program Capacity Development Workshop: Re-
15   gional Air Pollution Royal Princess Hotel, Bangkok, Thailand, http://www.atm.ncu.edu.tw/95/
ppt/, 8–10 October 2008.

Corrigan, C. E., Ramanathan, V., and Schauer, J. J.: Impact of monsoon transitions
on the physical and optical properties of aerosols, J. Geophys. Res., 111, D18208,
doi:10.1029/2005JD006370, 2006.

20   Dubovik, O. and King, M.: A flexible inversion algorithm for retrieval of aerosol optical properties
from Sun and sky radiance measurements, J. Geophys. Res., 105, 20673–20696, 2000.

Dubovik, O., Smirnov, A., Holben, B. N., Eck, T. F., King, M. D., Kaufman, Y. J., and Slutsker,
I.: Accuracy assessments of aerosol optical properties retrieved from Aerosol Robotic Net-
work (AERONET) Sun and sky radiance measurements, J. Geophys. Res., 105, 9791–9806,
25   2000.

Dubovik, O., Holben, B., Eck, T. F., Smirnov, A., Kaufman, Y. J., King, M. D., Tanré, D., and
Slutsker, I.: Variability of Absorption and Optical Properties of Key Aerosol Types Observed
in Worldwide Locations, J. Atmos. Sci., 59, 590–608, 2002.

ACPD

12, 18927–18958, 2012

Classification and investigation of Asian aerosol properties

T. Logan et al.

Title Page

Abstract	Introduction
Conclusions	References
Tables	Figures

|◀ | ▶|

◀ | ▶

Back | Close

Full Screen / Esc

Printer-friendly Version

Interactive Discussion

Eck, T. F., Holben, B. N., Reid, J. S., Dubovik, O., Smirnov, A., O'Neill, N. T., Slutsker, I., and Kinne, S.: Wavelength dependence of the optical depth of biomass burning, urban, and desert dust aerosols, J. Geophys. Res., 31333–31349, 1999.

Eck, T. F., Holben, B. N., Boonjawat, J., Snidvongs, A., Nguyen, A. X., Le, H. V., Schafer, J. S., Kamol, S., Meesiri, S., Kaewkonga, T., Mongkolnavin, R., Reid, J. S., Remer, L. A., Dubovik, O., and Smirnov, A.: Aerosol optical properties in Southeast Asia from AERONET observations, American Geophysical Union, Fall Meeting 2003, http://www.atm.ncu.edu.tw/95/ppt/NO3%20Brent%20Holben%20\&%20Tom%20Eck/SE_ASIA_Taiwan_sem2.pdf, 2003.

Eck, T. F., Holben, B. N., Dubovik, O., Smirnov, A., Goloub, P., Chen, H. B., Chatenet, B., Gomes, L., Zhang, X.-Y., Tsay, S.-C., Ji, Q., Giles, D., and Slutsker, I.: Columnar aerosol optical properties at AERONET sites in central eastern Asia and aerosol transport to the tropical mid-Pacific, J. Geophys. Res., 110, D06202, doi:10.1029/2004JD005274, 2005.

Eck, T. F., Holben, B. N., Sinyuk, A., Pinker, R. T., Goloub, P., Chen, H., Chatenet, B., Li, Z., Singh, R. P., Tripathi, S. N., Reid, J. S., Giles, D. M., Dubovik, O., O'Neill, N. T., Smirnov, A., Wang, P., and Xia, X.: Climatological aspects of the optical properties of fine/coarse mode aerosol mixtures, J. Geophys. Res., 115, D19205, doi:10.1029/2010JD014002, 2010.

Giles, D. M., Holben, B. N., Tripathi, S. N., Eck, T. F., Newcomb, W. W., Slutsker, I., Dickerson, R. R., Thompson, A. M., Mattoo, S., Wang, S.-H., Singh, R. P., Sinyuk, A., and Schafer, J. S.: Aerosol properties over the Indo-Gangetic Plain: A mesoscale perspective from the TIGERZ experiment, J. Geophys. Res., 116, D18203, doi:10.1029/2011JD015809, 2011.

Gobbi, G. P., Kaufman, Y. J., Koren, I., and Eck, T. F.: Classification of aerosol properties derived from AERONET direct sun data, Atmos. Chem. Phys., 7, 453–458, doi:10.5194/acp-7-453-2007, 2007.

Hansen, J. and Sato, M.: Trends of measured climate forcing agents, available at: http://pubs.giss.nasa.gov/docs/2001/2001_Hansen_Sato.pdf, 2001.

Higurashi, A. and Nakajima, T.: Detection of aerosol types over the East China Sea near Japan from four-channel satellite data, Geophys. Res. Let., 29, 1836, doi:10.1029/2002GL015357, 2002.

Huang, J., Minnis, P., Chen, B., Huang, Z., Liu, Z., Zhao, Q., Yi, Y., and Ayers, J. K.: Long-range transport and vertical structure of Asian dust from CALIPSO and surface measurements during PACDEX, J. Geophys. Res., 113, D23212, doi:10.1029/2008JD010620, 2008.

Holben, B. N., Eck, T. F., Slutsker, I., Tanré, D., Buis, J. P., Setzer, A., Vermote, E., Reagan, J. A., Kaufman, Y. J., Nakajima, T., Lavenu, F., Jankowiak, I., and Smirnov, A.: AERONET – A

Discussion Paper | Discussion Paper | Discussion Paper | Discussion Paper | Discussion Paper

federated instrument network and data archive for aerosol characterization, Remote Sens. Environ., 66, 1–16, 1998.

Holben, B. N., Eck, T. F., Slutsker, I., Smirnov, Sinyuk, A., Schafer, A. J., Giles, D., and Dubovik, O.: AERONET's version 2.0 quality assurance criteria, Remote Sensing of Atmosphere and Clouds, Proc. SPIE Int. Soc. Opt. Eng., 6408, 64080Q, doi:10.1117/12.706524, 2006.

Intergovernmental Panel on Climate Change: Climate Change 2007: The Physical Science Basis. Contribution of Working Group I to the Fourth Assessment Report of the Intergovernmental Panel on Climate Change, edited by: Solomon, S., Qin, D., Manning, M., Chen, Z., Marquis, M., Averyt, K. B., Tignor, M., and Miller, H. L., Cambridge Univ. Press, New York, 2007.

Jeong, J. I., Park, J., Woo, J.-H., Han, Y.-J., and Yi, S.-M.: Source contributions to carbonaceous aerosol concentrations in Korea, Atmos. Environ., 45, 1116–1125, 2011.

Jin, M. S., Kessomkiat, W., and Pereira, G.: Satellite-Observed Urbanization Characters in Shanghai, China: Aerosols, Urban Heat Island Effect, and Land-Atmosphere Interactions, Remote Sens., 3, 83–99, doi:10.3390/rs3010083, 2011.

Kaufman, Y. J., Tanré D., and Boucher, O.: A satellite view of aerosols in the climate system, Nature, 419, 215–223, doi:10.1038/nature01091, 2002.

Kondo, Y., Matsui, H., Moteki, N., Sahu, L., Takegawa, N., Kajino, M., Zhao, Y., Cubison, M. J., Jimenez, J. L., Vay, S., Diskin, G. S., Anderson, B., Wisthaler, A., Mikoviny, T., Fuelberg, H. E., Blake, D. R., Huey, G., Weinheimer, A. J., Knapp, D. J., and Brune, W. H.: Emissions of black carbon, organic, and inorganic aerosols from biomass burning in North America and Asia in 2008, J. Geophys. Res., 116, D08204. doi:10.1029/2010JD015152, 2011.

Koven, C. D. and I. Fung.: Inferring dust composition from wavelength-dependent absorption in Aerosol Robotic Network (AERONET) data, J. Geophys. Res., 111, D14205, doi:10.1029/2005JD006678, 2006.

Lack, D. A. and Cappa, C. D.: Impact of brown and clear carbon on light absorption enhancement, single scatter albedo and absorption wavelength dependence of black carbon, Atmos. Chem. Phys., 10, 4207–4220, doi:10.5194/acp-10-4207-2010, 2010.

Levin, Z., Ganor, E., and Gladstein, V.: The effects of desert particles coated with sulfate on rain formation in the eastern Mediterranean, J. App. Meteor., 35, 1511–1523, 1996.

Lewis, K., Arnott, W. P., Moosmüller, H., and Wold, C. E.: Strong spectral variation of biomass smoke light absorption and single scattering albedo observed with a novel dual-wavelength

photoacoustic instrument, J. Geophys. Res., 113, D16203. doi:10.1029/2007JD009699, 2008.

Li, Z., Chen, H., Cribb, M., Dickerson, R., Holben, B., Li, C., Lu, D., Luo, Y., Maring, H., Shi, G., Tsay, S.-C., Wang, P., Wang, Y., Xia, X., Zheng, Y., Yuan, T., and Zhao, F.: Aerosol optical properties and its radiative effects in northern China, J., Geophys. Res., 112, D22S01. doi:10.1029/2006JD007382, 2007a.

Li, Z., Chen, H., Cribb, M., Dickerson, R., Holben, B., Li, C., Lu, D., Luo, Y., Maring, H., and Shi, G.: Preface to special section on East Asian Studies of Tropospheric Aerosols: An International Regional Experiment (EAST-AIRE), J. Geophys. Res., 112, D22S00. doi:10.1029/2007JD008853, 2007b.

Logan, T., Xi, B., Dong, X., Obrecht, R., Li, Z., and Cribb, M.: A study of Asian dust plumes using satellite, surface, and aircraft measurements during the INTEX-B field experiment, J. Geophys. Res., 115, D00K25. doi:10.1029/2010JD014134, 2010.

Pan, L., Che, H., Geng, F., Xia, X., Wang, Y., Zhu, C., Chen, M., Gao, W., and Guo, J.: Aerosol optical properties based on ground measurements over the Chinese Yangtze Delta Region, Atmos. Environ., 44, 2587–2596, 2010.

Pathak, R. K., Wu, W. S., and Wang, T.: Summertime PM2.5 ionic species in four major cities of China: nitrate formation in an ammonia-deficient atmosphere, Atmos. Chem. Phys., 9, 1711-1722, doi:10.5194/acp-9-1711-2009, 2009.

Reid, J. S., Eck, T. F., Christopher, S. A., Hobbs P. V., and Holben, B.: Use of the Angström exponent to estimate the variability of optical and physical properties of aging smoke particles in Brazil, J. Geophys. Res., 104, 27473–27489, 1999.

Russell, P. B., Bergstrom, R. W., Shinozuka, Y., Clarke, A. D., DeCarlo, P. F., Jimenez, J. L., Livingston, J. M., Redemann, J., Dubovik, O., and Strawa, A.: Absorption Angstrom Exponent in AERONET and related data as an indicator of aerosol composition, Atmos. Chem. Phys., 10, 1155–1169, doi:10.5194/acp-10-1155-2010, 2010.

Schuster, G. L., Dubovik, O., Holben, B. N., and Clothiaux, E. E.: Inferring black carbon content and specific absorption from Aerosol Robotic Network (AERONET) aerosol retrievals, J. Geophys. Res., 110, D10S17. doi:10.1029/2004JD004548, 2005.

Schuster, G. L., Dubovik, O., and Holben, B. N.: Angstrom exponent and bimodal aerosol size distributions, J. Geophys. Res., 111, D07207, doi:10.1029/2005JD006328, 2006.

Classification and investigation of Asian aerosol properties

T. Logan et al.

Title Page

Abstract	Introduction
Conclusions	References
Tables	Figures

◄◄ | ►►

◄ | ►

Back | Close

Full Screen / Esc

Printer-friendly Version

Interactive Discussion

Streets, D. G., Fu, J. S., Jang, C. J., Hao, J., Kebin, H., Tang, X., Zhang, Y., Wang, Z., Li, Z., Zhang, Q., Wang, L., Wang, B., and Yu, C.: Air quality during the 2008 Beijing Olympic Games, Atmos. Environ., 41, 480–492, 2007.

Wang, Y., Xin, J., Li, Z., Wang, S., Wang, P., Hao, W. M., Nordgren, B. L., Chen, H., Wang, L., and Sun, Y.: Seasonal variations in aerosol optical properties over China, Atmos. Chem. Phys. Discuss., 8, 8431–8453, doi:10.5194/acpd-8-8431-2008, 2008.

Xin, J., Wang, Y., Li, Z., Wang, P., Hao, W. M., Nordgren, B. L., Wang, S., Liu, G., Wang L., Wen T., Sun Y., and Hu, B.: Aerosol optical depth (AOD) and ?ngström exponent of aerosols observed by the Chinese Sun Hazemeter Network from August 2004 to September 2005, J. Geophys. Res., 112, D05203. doi:10.1029/2006JD007075, 2007.

Yao, X., Chan, C. K., Fang, M., Cadle, S., Chan, T., Mulawa, P., He, K., and Ye, B.: The water-soluble ionic composition of $PM_{2.5}$ in Shanghai and Beijing, China, Atmos. Environ., 36, 4223–4234, 2002.

Yoon, S.-C., Kang, J.-Y., and Goto, D.: Estimation of mineral dust emission in East Asia, SALSA Workshop AORI, UT, 15 December, 2011

Zheng, M., Salmon, L. G., Schauer, J. J., Zeng, L., Kiang, C. S., Zhang, Y., and Cass, G. R.: Seasonal trends in $PM_{2.5}$ source contributions in Beijing, China, Atmos. Environ., 39, 3967–3976, 2005.

Table 1. Summary of statistical data from the four AERONET sites. Yearly means of r_{eff} are calculated from the seasonal mean values due to an uneven distribution of seasonal data.

		Xianghe		Mukdahan		Taihu		SACOL	
		For ω_o; $\tau_{440nm} > 0.4$		For ω_o; $\tau_{440nm} > 0.4$		For ω_o; $\tau_{440nm} > 0.4$		For ω_o; $\tau_{440nm} > 0.4$	
		mean (σ)	N^a	mean (σ)	N	mean (σ)	N	mean (σ)	N
Year	τ_{440nm}	1.10 (0.60)	688	0.80 (0.31)	394	0.93 (0.43)	435	0.63 (0.28)	292
	$\tau_{abs440nm}$	0.10 (0.05)		0.07 (0.03)		0.09 (0.04)		0.05 (0.03)	
	$\alpha_{440-870nm}$	1.12 (0.32)		1.51 (0.18)		1.19 (0.28)		0.78 (0.38)	
	$\alpha_{abs440-870nm}$	1.53 (0.39)		1.14 (0.29)		1.49 (0.37)		1.32 (0.49)	
	$\alpha(\omega_{oabs440-870nm})$	0.41 (0.61)		−0.37 (0.26)		0.29 (0.55)		0.54 (0.76)	
	r_{eff} (fine mode)	0.17		0.18		0.17		0.16	
	r_{eff} (coarse mode)	2.26		2.51		2.19		2.05	
Spring	τ_{440nm}	1.02 (0.55)	198	0.87 (0.33)	191	0.88 (0.36)	162	0.69 (0.34)	108
	$\tau_{abs440nm}$	0.10 (0.05)		0.07 (0.03)		0.08 (0.04)		0.06 (0.03)	
	$\alpha_{440-870nm}$	0.93 (0.40)		1.58 (0.15)		1.05 (0.33)		0.47 (0.34)	
	$\alpha_{abs440-870nm}$	1.67 (0.45)		1.24 (0.26)		1.58 (0.38)		1.52 (0.56)	
	$\alpha(\omega_{oabs440-870nm})$	0.74 (0.76)		−0.35 (0.26)		0.53 (0.63)		1.05 (0.81)	
	r_{eff} (fine mode)	0.15 (0.03)		0.16 (0.02)		0.15 (0.03)		0.13 (0.04)	
	r_{eff} (coarse mode)	2.15 (0.28)		2.47 (0.42)		1.92 (0.25)		1.82 (0.23)	
Summer	τ_{440nm}	1.28 (0.73)	147	n/a^b	n/a	1.32 (0.61)	36	0.68 (0.39)	36
	$\tau_{abs440nm}$	0.06 (0.04)		n/a		0.08 (0.04)		0.04 (0.02)	
	$\alpha_{440-870nm}$	1.24 (0.24)		n/a		1.27 (0.23)		1.01 (0.33)	
	$\alpha_{abs440-870nm}$	1.39 (0.38)		n/a		1.37 (0.57)		1.30 (0.48)	
	$\alpha(\omega_{oabs440-870nm})$	0.15 (0.48)		n/a		0.10 (0.63)		0.29 (0.68)	
	r_{eff} (fine mode)	0.20 (0.05)		n/a		0.21 (0.04)		0.19 (0.05)	
	r_{eff} (coarse mode)	2.43 (0.26)		n/a		2.49 (0.34)		2.01 (0.44)	
Autumn	τ_{440nm}	1.04 (0.57)	180	0.70 (0.27)	63	0.91 (0.46)	126	0.53 (0.12)	48
	$\tau_{abs440nm}$	0.10 (0.04)		0.04 (0.02)		0.07 (0.04)		0.04 (0.01)	
	$\alpha_{440-870nm}$	1.22 (0.23)		1.36 (0.18)		1.34 (0.18)		1.09 (0.15)	
	$\alpha_{abs440-870nm}$	1.41 (0.28)		0.97 (0.39)		1.41 (0.34)		1.18 (0.48)	
	$\alpha(\omega_{oabs440-870nm})$	0.18 (0.40)		−0.39 (0.34)		0.07 (0.43)		0.09 (0.53)	
	r_{eff} (fine mode)	0.17 (0.04)		0.21 (0.02)		0.18 (0.03)		0.19 (0.03)	
	r_{eff} (coarse mode)	2.30 (0.22)		2.58 (0.37)		2.33 (0.27)		2.24 (0.35)	
Winter	τ_{440nm}	1.09 (0.54)	163	0.73 (0.27)	140	0.88 (0.38)	111	0.60 (0.17)	100
	$\tau_{abs440nm}$	0.12 (0.05)		0.07 (0.03)		0.10 (0.04)		0.05 (0.02)	
	$\alpha_{440-870nm}$	1.14 (0.26)		1.47 (0.16)		1.21 (0.22)		0.89 (0.27)	
	$\alpha_{abs440-870nm}$	1.62 (0.36)		1.09 (0.22)		1.47 (0.26)		1.19 (0.32)	
	$\alpha(\omega_{oabs440-870nm})$	0.48 (0.47)		−0.38 (0.19)		0.26 (0.37)		0.30 (0.48)	
	r_{eff} (fine mode)	0.17 (0.04)		0.17 (0.02)		0.18 (0.04)		0.18 (0.04)	
	r_{eff} (coarse mode)	2.18 (0.24)		2.51 (0.43)		2.31 (0.24)		2.23 (0.34)	

[a] Number of AERONET observations.
[b] Only one data point for this season.

Fig. 1. Four selected AERONET observational sites used in this study. Note the proximities of Xianghe, SACOL and Taihu to the Gobi and Taklimakan deserts while Mukdahan is not near any desert or large urban areas.
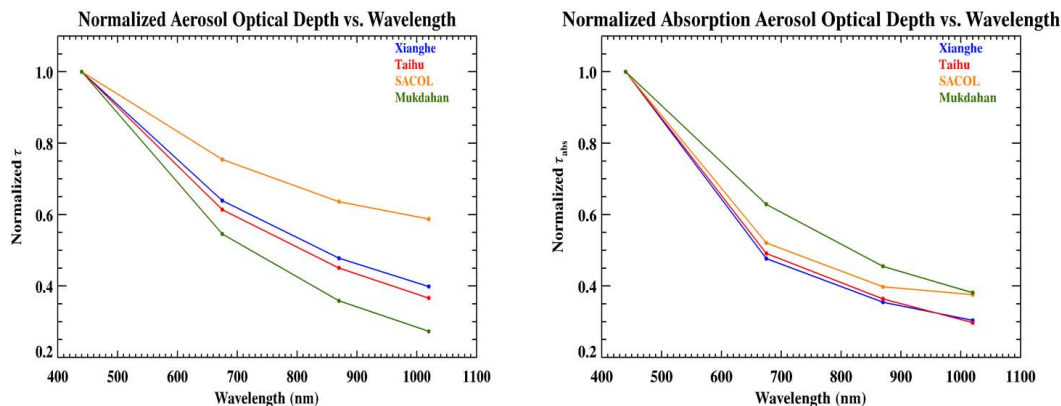
Fig. 2. Statistical results of normalized aerosol extinction and absorption optical depths retrieved from the four selected AERNET sites. All values are normalized to τ_{440} and τ_{abs440} following the methodology of Yoon et al. (2011).

Fig. 3. Aerosol size distributions over the four selected AERONET sites. **(a)** Annual and **(b–e)** seasonal means (standard deviation) of aerosol optical depth (τ) and Ångström exponent (α) were calculated using data during the periods: 2001–2010 (Xianghe), 2005–2010 (Taihu), 2006–2011 (SACOL), and 2003–2009 (Mukdahan). Note that there is no summer result at Mukdahan due to limited observations of aerosols.

Title Page

Abstract | Introduction

Conclusions | References

Tables | Figures

◄ | ►

Back | Close

Full Screen / Esc

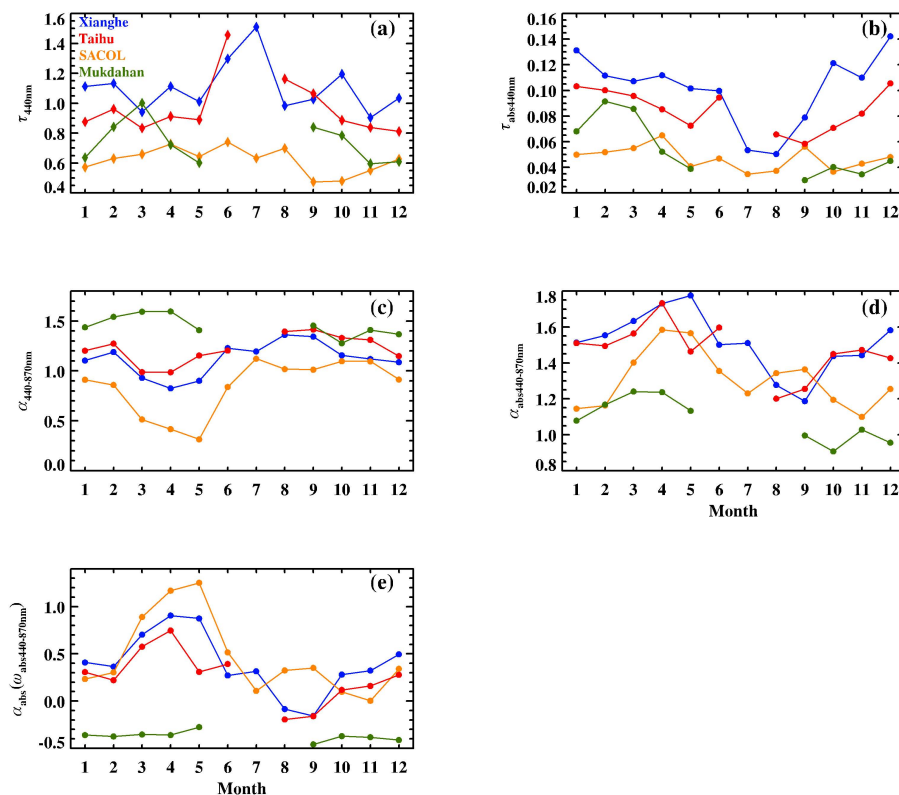Printer-friendly Version

Interactive Discussion

Fig. 4. Monthly means of the five parameters used in this study. Note that the missing monthly means at Taihu and Mukdahan are due to limited observations of aerosols during prolonged wet periods (summer season).

Title Page

Abstract | Introduction

Conclusions | References

Tables | Figures

◄ | ►

◄ | ►

Back | Close

Full Screen / Esc

Printer-friendly Version

Interactive Discussion

Classification and investigation of Asian aerosol properties
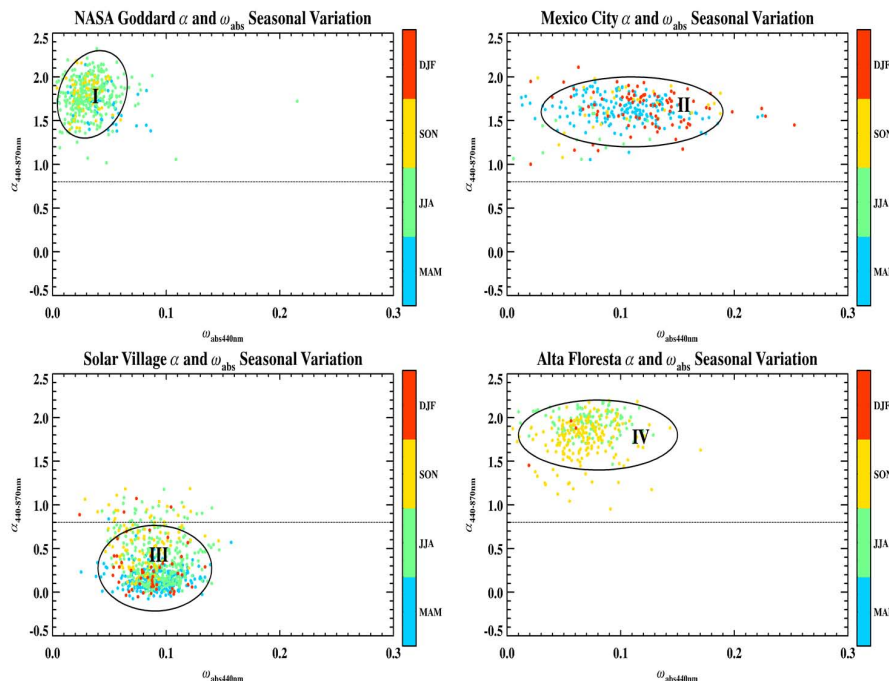
T. Logan et al.

Fig. 5. Cluster analysis of four additional AERONET sites representing pollution (NASA Goddard and Mexico City), mineral dust (Solar Village) and biomass (Alta Floresta) aerosol types. A threshold of α = 0.8 is used to define the fine (> 0.8) and coarse (< 0.8) mode aerosols, while weakly (ω_{abs} < 0.07) and strongly (ω_{abs} > 0.07) absorbing aerosols are set at ω_{abs} = 0.07. Note the small seasonal variability in aerosol type among the three of the four sites indicating a primary single aerosol influence. Solar Village is near Riyadh, Saudi Arabia, primarily dominated by mineral dust aerosols but occasionally influenced by urban aerosols.
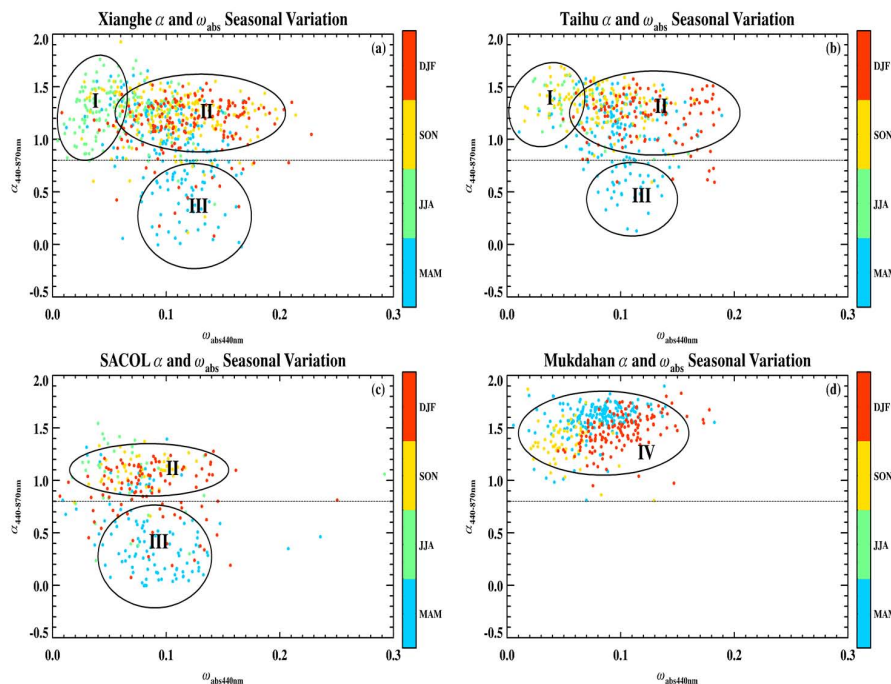
Fig. 6. Cluster analysis of the aerosol properties over the four selected AERONET sites. The data are color coded according to season to show correlations between aerosol composition/type and time of year.

Classification and investigation of Asian aerosol properties

T. Logan et al.

Title Page

Abstract | Introduction

Conclusions | References

Tables | Figures

⏮ | ⏭

◀ | ▶

Back | Close

Full Screen / Esc

Printer-friendly Version

Interactive Discussion